RAQUEL RAINIER ALVES SOARES

ELECTROCHEMICAL BIOSENSORS BASED ON LASER INDUCED GRAPHENE TO DETECT FOODBORNE PATHOGENS IN FOOD

Dissertation submitted to the Universidade Federal de Vicosa as part of requeriments of the Food Science and Technology Graduate Program, to obtain the title of *Magister Scientiae*.

VICOSA
MINAS GERAIS - BRAZIL
2019

Ficha catalográfica preparada pela Biblioteca Central da Universidade Federal de Viçosa - Campus Viçosa

T

S676e
2019

Soares, Raquel Rainier Alves, 1993-
Electrochemical biosensors based on laser induced graphene to detect foodborne pathogens in food / Raquel Rainier Alves Soares. - Vicosa, MG, 2019.
xi, 37f. : il. (algumas color.) ; 29 cm.

Texto em inglês.
Inclui apêndice.
Orientador: Nilda de Fatima Ferreira Soares.
Dissertação (mestrado) - Universidade Federal de Viçosa.
Referências bibliográficas: f.28-35.

1. Alimentos - Análise. 2. *Salmonella enterica*. 3. Segurança alimentar. 4. Análise eletroquímica. 5. Microscopia eletrônica. 6. Raman, Espectroscopia de. I. Universidade Federal de Viçosa. Departamento de Tecnologia de Alimentos. Programa de Pós-Graduação em Ciência e Tecnologia de Alimentos. II. Título.

CDD 22 ed. 664.07

RAQUEL RAINIER ALVES SOARES

ELECTROCHEMICAL BIOSENSORS BASED ON LASER INDUCED GRAPHENE TO DETECT FOODBORNE PATHOGENS IN FOOD

Dissertation submitted to the Universidade Federal de Vicosa as part of requeriments of the Food Science and Technology Graduate Program, to obtain the title of *Magister Scientiae.*

APPROVED: June 28th, 2019.

Carmen Luiza F. de Lima Gomes
(Co-advisor)

Efraim Lázaro Reis
(Co-advisor)

Luciano de Moura Guimarães

Nilda de Fátima Ferreira Soares
(Advisor)

“Without dreams, the losses become unbearable,
the stones on the road become mountains,
the failures turn into fatal blows.
But if you have big dreams ...
Your mistakes will produce growth,
your challenges will produce opportunities,
your fears will produce courage ...”

Augusto Cury

ACKNOWLEDGMENTS

Eu dedico a obtenção deste título aos meus pais. Agradeço ao meu pai Adil, com quem compartilhei o sonho de chegar até aqui, meu maior exemplo e inspiração que lutou para um dia me ver alfabetizada e agora pôde ver eu me tornar mestre. Agradeço à minha mãe Antonina, exemplo de mãe, meu anjo da guarda que não mede esforços para me apoiar e me ajudar, e acompanhou toda a minha trajetória com muito carinho. O amor de vocês é essencial para mim.

Aos meus irmãos, meus avós e todos os familiares pela união, pelos valores e por serem a minha razão para seguir em frente. À prima e amiga Débora por ter me mostrado que eu poderia realizar um grande sonho, como o fiz. Ao Fredy pelo companheirismo, por ter estado ao meu lado me apoiando sempre que eu precisei, engrandecendo o meu trabalho, valorizando o meu esforço, cuidando de mim, e claro, pelas demasiadas ajudas na contagem de bactérias nos finais de semana. Ao Departamento de Tecnologia de Alimentos, pela oportunidade de desenvolvimento como pessoa e aluno, assim como ao CNPq, pela concessão da bolsa de estudos e aprovação de estágio no exterior.

Aos membros do Laboratório de Embalagens, Taíla, Nelson, Michele, Eber, Alane, Laís, José, Rafael, Rafaela, Adassa e Miriane pelo companheirismo do dia a dia e amizade, em especial ao Pedro que me ajudou muito, compartilhando material, conhecimento, palpites e sonhos sem medir esforços para me ajudar, assim como não poderia deixar de agradecer aos amigos do laboratório de Iowa, Kshama, Juliana, Cícero e Gage pela amizade e ajuda indescritível.

Agradeço à professora Nilda pela orientação e apoio para executar o trabalho no exterior, à co-orientadora Carmen por ter me acolhido tão bem em seu laboratório, me apoiado desde o início, e me ajudado a concretizar este sonho, ao co-orientador Efraim por ter abraçado este projeto desde o início com muito entusiasmo, pelo suporte sempre quando necessário, e pelas dicas valiosas que foram muito bem empregadas. Vocês são exemplos de profissionais que levarei para sempre comigo. Aos professores Luciano, Sukarno e Renê que me ajudaram a conduzir análises no Departamento de Física com muita prestatividade.

A todos os meus queridos amigos que contribuíram para que eu cumprisse esta etapa desafiadora em minha vida. Esta vitória é minha graças a todos vocês! O meu muito obrigada.

BIOGRAPHY

RAQUEL RAINIER ALVES SOARES, daughter of Adil Rainier Alves and Maria Antonina Soares Alves, was born in Capitolio, Brazil, on June 3rd, 1993. She attended her junior and secondary education at Colegio Anglo de Vicosa. As soon as she completed her basic education, she joined the Universidade Federal de Vicosa and obtained a B.S. degree in Food Engineering in 2017. She has had experience in Food Packaging with emphasis on Active Packaging, mainly on antimicrobial and biodegradable films, with a specialization in Packaging and Conditioning at the Universite de Lorraine (2015), France. After her undergraduate studies, she joined the Graduate Program in Food Science and Technology at the Universidade Federal de Vicosa, carried out the project at the Iowa State University and submitted her dissertation to be defended in June.

LIST OF FIGURES

LIST OF TABLES

LIST OF ABBREVIATIONS

Ag – Silver

AgCl – Silver chloride

ATCC – American Type Culture Collection

AuNPs – Gold Nanoparticles

BPW – Buffered Peptone Water

CA – Chronoamperometry

C_{dl} – Double-layer capacitance

CFU – Colony forming unit

CNTs – Carbon Nanotubes

CV – Cyclic Voltammetry

DPV – Differential Pulse Voltammetry

DWE – Double-Walled Electrode

EDC – 1-Ethyl-3-(3-dimethylaminopropyl) carbodiimide

EDS – Energy dispersive spectroscopy

EIS – Electrochemical Impedance Spectroscopy

ELISA – Enzyme-linked immunosorbent assays

EPPG – Edge plane pyrolytic graphite

ESA – Electrochemical surface area

FDA – Food and Drug Administration

GCE – Glassy Carbon Electrodes

GO – Graphene oxyde

HET – Heterogeneous electron transfer

HOPG – Highly ordered pyrolytic graphite

I – Impedimetry

IME – Interdigitated Microelectrode

IS – Impedance Spectroscopy

ISE – Ion Selective Electrodes

KCl – Potassium chloride

LCVD – Laser chemical vapor deposition

LDW – Laser direct writing

LIG – Laser induced graphene

LOD – Limit of detection

MES – 2-(N-morpholino) ethanesulfonic acid

MSNTs – Magnetic Silica Nanotubes

NHS – N-hidroxissuccinimida

P – Potentiometry

PBS – Phosphate buffered saline

PCR – Polymerase chain reaction

PI – Polyimide

R_{ct} – Charge transfer resistance

rGO – Reduced graphene oxyde

R_s – Solution resistance

SD – Standart deviation

SPE – Screen-Printed Electrodes,

SP-IDME –Interdigitated Microelectrode

TSA/TSB – Tryptic soy agar / Tryptic soy broth

TVC – Total viable counts

UN – United Nations

USDA – U.S. Department of Agriculture

XRD – X-Ray Diffraction

Z_W – Warburg impedance element

ΔE_p – Potential variation among peaks

ABSTRACT

SOARES, Raquel Rainier Alves, M.Sc., Universidade Federal de Vicosa, June, 2019. **Electrochemical biosensors based on Laser Induced Graphene to detect foodborne pathogens in food.** Advisor: Nilda de Fátima Ferreira Soares. Co-advisors: Carmen Luiza Feitosa de Lima Gomes and Efraim Lázaro Reis.

With the sharp increase in the world population, the demand for food production with an efficient quality control has grown substantially, since foodborne diseases and contaminations still considerably impact society. Therefore, there is a serious need for rapid, easy handling, sensitive and inexpensive biosensor devices, considered to be an excellent alternative to monitor food quality. Linked to this, researches on materials that are eco-friendly, easy to obtain, simple handling and widely applicable have become increasingly present in the scope of innovation and development of new products, such as graphene. In this context, the objective of this work is to develop electrochemical biosensors based on graphene produced by laser induction, incorporated with specific antibodies to detect *Salmonella enterica*, and to apply them on food. Firstly, porous graphene electrodes were obtained by Laser-Induced Graphene (LIG) and evaluated according to its morphology, electrical conductivity, charge transfer ability, and graphene formation quality. The characterization techniques employed were: Scanning Electron Microscopy, Cyclic Voltammetry, Raman Spectroscopy and X-Ray Diffraction (XRD). The electrodes displayed good electrochemical performance, and were sequentially incorporated with antibodies, thus obtaining immunosensors. These devices showed excellent ability to detect pathogenic bacteria in food using the Electrochemical Impedance Spectroscopy technique, which represents an important advance in the field of food safety. Finally, the selectivity of the immunosensor was also tested in food using another inoculated pathogen, *Escherichia coli*, under the same conditions, playing the role of a negative control. Considered a highly promising device that can be easily produced, the developed impedimetric immunosensor has unique properties that make it a viable option for pathogen detection in food, and an excellent alternative for electrochemical sensors that are directly induced onto the film.

RESUMO

SOARES, Raquel Rainier Alves, M.Sc., Universidade Federal de Vicosa, junho de 2019. **Biossensores eletroquímicos à base de grafeno produzido a laser para detectar patógenos em alimentos.** Orientadora: Nilda de Fátima Ferreira Soares. Coorientadores: Carmen Luiza Feitosa de Lima Gomes e Efraim Lázaro Reis.

Com o aumento acentuado da população, a demanda por produção de alimentos cresceu substancialmente, atrelada à necessidade de um eficiente controle de qualidade, visto que doenças e contaminações transmitidas por alimentos ainda impactam substancialmente a sociedade. Portanto, existe uma grande necessidade de desenvolver sensores rápidos, fáceis de operar, sensíveis e baratos, como uma excelente alternativa para o monitoramento da qualidade dos alimentos. Associado a isto, a busca por materiais ecologicamente corretos, de fácil obtenção, simples manuseio e ampla aplicabilidade tem se tornado cada vez mais presente no âmbito da inovação e desenvolvimento de novos produtos, como é o caso do grafeno. Neste contexto, o objetivo deste trabalho foi desenvolver biossensores eletroquímicos à base de grafeno produzido por indução a laser, incorporados com anticorpos específicos para detectar *Salmonella enterica*, e aplicar em alimentos. Primeiramente, os eletrodos à base de grafeno poroso foram obtidos pela ténica *Laser-Induced Graphene* (LIG) e avaliados quanto à morfologia, condutividade elétrica, capacidade de transferência de carga, e qualidade da formação do grafeno. As ténicas de caracterização empregadas para tal foram Microscopia Eletrônica de Varredura, Voltametria Cíclica, Espectroscopia Raman e Difração de Raio-X. Os eletrodos apresentaram bom desempenho eletroquímico, e sequencialmente foram incorporados com anticorpos, obtendo-se assim, imunossensores. Tais dispositivos apresentaram excelente capacidade de detecção de bactéria patogênica em alimento por meio da técnica Espectroscopia de Impedância Eletroquímica, o que representa um importante avanço no campo de alimento seguro. Por fim, a seletividade do imunossensor foi testada também em alimento, porém com outro patógeno inoculado, no caso *Escherichia coli* nas mesmas condições, atuando como controle negativo. Considerado um dispositivo altamente promissor, que pode ser facilmente produzido, o imunossensor impedimétrico desenvolvido possui propriedades ímpares que o tornam uma opção viável para detecção de patógenos em alimentos, e uma excelente plataforma para sensores eletroquímicos impressos diretamente.

SUMMARY

1. General Introduction

Nearly half a million people die each year from acquiring foodborne illnesses[1]. Usual techniques used to detect pathogens, such as Total Viable Counts (TVC), Polymerase Chain Reaction (PCR), and Enzyme-Linked Immunosorbent Assays (ELISA), are time-consuming and relatively expensive, since they require laboratory analyses performed by trained personnel[2]. Thereby, foodborne pathogen detection in processing facilities is inadequately performed due to cost, time and specific execution requirements; for instance, the sample pre-enrichment obtained by laboratory techniques[3].

The origin of foodborne pathogen outbreaks is often unknown or difficult to accurately identify. Nevertheless, a low-cost, on-site, rapid, direct, highly sensitive, and reliable method for this purpose currently does not exist. An alternative to improve routine analyses is the development of biosensors. Biosensors have been considerably studied for the past years since they are seen as an alternative to traditional methods of pathogen detection, mainly due to their fast response, high specificity and sensitivity[2,4]. This new branch of devices can be classified in several ways. One of these classifications is impedimetric immunosensors; biosensors which have the impedance as the transduction technique and antibodies as the specific bioreceptors[4,5]. They have been receiving particular attention, since they confer direct and label-free measurements, and can be easily manipulated[6,7].

This emerging field presents a variety of devices that promise to overcome the limitations of existing detection methods. Ensuring greater food quality control contributes to reduce these restrictions, even though strict regulations have still enabled huge disease outbreaks to occur[8], historically. Therefore, there is a critical need to develop rapid and viable sensors in order to reduce costs and time of food contamination monitoring within the facilities.

Electrochemical analysis systems that combine electrochemical transducers with specific bioreceptors offer both sensitivity and rapidity needed for in-plant monitoring[9]. Disposable and direct sensing devices provide a rapid bioconjugation between the target analyte and the biorecognition agent, since they reduce the response time of a pre-treatment necessity evaluation. The goal of this work is to develop and validate an electrochemical biosensor from a promising graphene production technique incorporated with antibodies as the bioreceptors for the detection of *Salmonella enterica*, one of the most critical foodborne pathogens, directly on the food.

Graphene and graphene-like nanomaterials have stimulated several research groups the

past years due to their unique properties[10]. Numerous studies have approached these materials as a great potential for electrochemical transducers, since they present excellent electrical conductivity[11,12]. Through this biosensing system the bacteria can be monitored by specific recognition from particles of the receptor biomolecule and accurate pathogen detection is provided. The main idea is that the combination of a material with great electrical properties, like graphene, and a very specific recognition molecule, like an antibody, would provide an electrochemical sensor highly sensitive for the detection of foodborne pathogens. This hypothesis was formulated based on previous works[13–15] that demonstrated that laser induction on commercial polymers can produce porous graphene with several properties of interest, and other works that demonstrated very selective immunosensors[16–18]. Furthermore, the laser process is amenable to a fabrication using low-cost, disposable and flexible materials.

The rationale for the proposed device is that its success would reflect to an innovative rapid detection method which would improve both temporal and spatial monitoring of foodborne pathogen contamination on-site, inexpensively, with no requirements of trained personnel. Then, its sensitivity would be comparable to current techniques for *Salmonella* detection, as outlined by the USDA Food Safety and Inspection Service[8]. In addition to this appeal to food safety, this immunosensor is made of an emerging material, graphene, which has several properties that make it interesting for wide different applications as well.

This work contains the following specific aims: 1) To produce and characterize highly feasible electrodes based on laser-induced graphene technique; 2) To functionalize the bare electrode with specific antibody for *Salmonella enterica* detection; 3) To validate the immunosensor through the impedimetric technique, by applying it on real food.

2. Review of Literature

2.1. Laser Induced Graphene

The discovery of nanomaterials based on carbon has boosted researchers to develop a novel carbon-based nanotechnology, since they provide a wide potencial of application. Over the past decades, graphene, one of these materials, has attracted tremendous attention both in research and industry fields, due to its peculiar features[15]. Graphene is a sheet of sp^2 bonded carbon atoms arranged into a rigid hexagonal lattice exhibiting application in engineering, physics, chemistry, and materials science, due to its superior and atypical properties, including large surface area, electron transfer capability, thermal conductivity, excellent mechanical properties, biocompatibility, among others[19–23]. These unique abilities make graphene a great potential material with promising applications in electrochemical biosensors, supercapacitors, microelectronics, and energy storage[24–28].

Thereby, alternative methodes for synthesis of graphene has expanded substantially, confirmed by the emergence of several techniques. However, the cost of the synthesis and implementation are still a challenge, which restricts its applications[29]. Most of them require conductive graphene films or coatings with particular shapes and sizes. Therefore, attempts have been made to pattern graphene onto various substrates, for example, printing techniques like screen printing and inkjet printing[30]. However, these methods usually have limitations like expensive instruments, complicated operations or need of extra templates[29]. Proceeding this high demand, the synthesis of carbon nanomaterials from inexpensive precursors using cost-effective processes is highly required for industrial production[31,32]. They search graphene with high carrier mobility, conductivity, stiffness, and electrochemical properties. Recently, Tour et al.[33] from Rice University developed a simple and effective method to produce porous graphene from commercial polyimide films by laser induction under ambient conditions. In their study, the produced material named laser-induced graphene (LIG) was described as containing few-layer graphene with high electrical and thermal conductivity, and excellent electrochemical performance[34].

Initially, Kaner group[35] introduced this initial idea of laser-induction promoting reduction of graphene oxide (GO) films through LightScribe DVD optical drive, which produced graphene with great electrochemical properties. Few years later, Tour group[33] developed a direct method for LIG fabrication by laser-induced graphitization from polymers

such as polyimide (PI) at high temperature. In recent years, laser direct writing (LDW) technique has provided a powerful processing method for the broad application of LIG with no ultra high temperature or toxic chemicals[22]. Porous graphene has been successfully formed on PI films using a CO_2 infrared laser under ambient conditions[33].

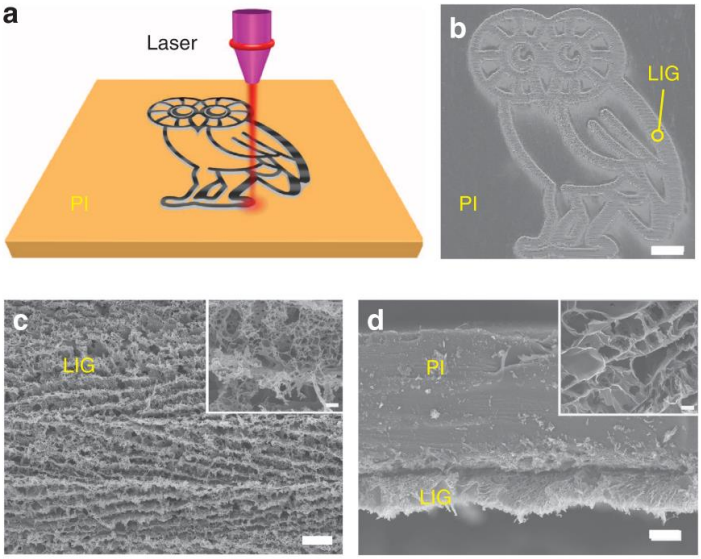

Figure 1. LIG formed from polyimide film using a CO_2 laser. Image obtained and adapted from[33].

Comparing traditional processing methods, such as mask lithography[36,37], direct-printing[30,38], laser processing[34,39], the LDW approach confers many advantages such as maskless, catalyst free, non-toxicity, controllability and non-contact[22]. One of the most important features of this direct technique is the flexibility and wide functionalization possibility at low cost[40]. The precursors commonly used to produce graphene through laser irradiation, for example conventional polymers, can be directly converted in graphene onto selected areas. Thereby, the structural morphology and properties of LIG are influenced by changing the laser parameters[39,41]. This can be confirmed from the work of Huang et al.[42] which demonstrated that graphene structure can be modified by low power density of CO_2 laser irradiation (2 to 60 W cm^{-2}). They showed that when the power density was low, crystalline graphene disassembled into nanocrystalline structure, and when the power density increased, amorphous carbon formed on the surface. At continuous conditions, laser-induced damage to graphene depends on the irradiated laser power and the exposure time, since thermal effect played an important role during the laser process[22]. For very fast laser, the laser-induced

damages are provoked without drastically changing the regions of graphene. As an example, Lin et al.[43] demonstrated an ultra rapid laser that formed multi-layered graphene with the desired layer number when appropriate pulse energy was adopted.

Laser processing of graphene is of great interest for engineering purposes. However, currently laser induction of graphene is still recent, requiring some improvements in order to tune properties and become more applicable. Therefore, it is very important to understand the graphene formation mechanism that occurs by induction laser process, and the variations that interfere in the quality of the obtained material. The laser-induced mechanism involves at least two steps that are mediated by distinct physical processes; one is the photochemical removal of oxygen from the GO surface, accompanied by laser ablation, and the other is structural reorganization of the newly reduced graphene structure, into planar and hexagonal structure[44].

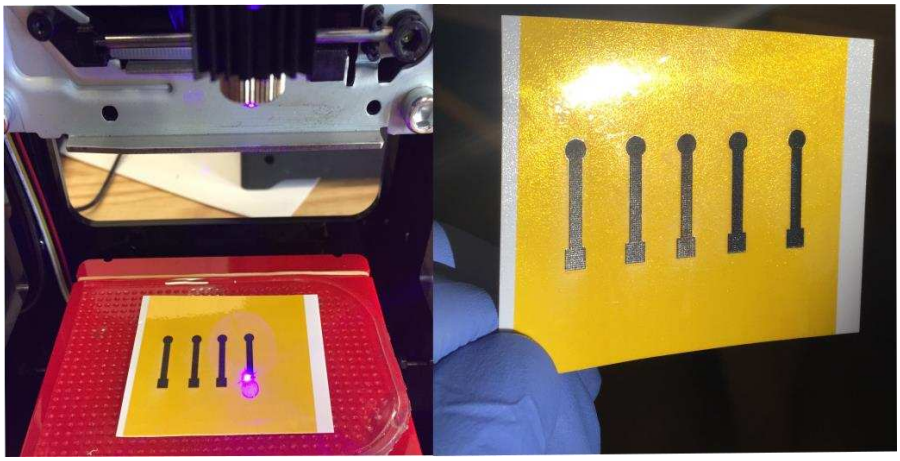

Figure 2. LIG-based electrodes produced from UV Laser under ambient conditions.

In addition to the previously cited methods, graphene can also be formed from various carbon source by laser-based technique. For example, the conversion of highly ordered pyrolytic graphite (HOPG) into graphene by laser exfoliation[45]; rapid single-step fabrication of graphene patterns using laser chemical vapor deposition (LCVD)[46] with large rate of graphene formation owing to the rapid heating and cooling mechanism; and laser reduction of graphene oxide (GO) producing reduced graphene oxide (rGO) films with a much higher conductivity, which attracts increasing attention as an alternative route to produce rGO films[35,47].

Studies reveal that the oxygen present in the air has a small effect on the oxidation of the laser ablation zone[15,48]. Therefore, large-scale conductive carbon materials can be fabricated

using LDW technique under ambient conditions without the need for inert atmospheres or chemical vapor deposition. These methods provide great possibility for the transformation of carbon sources into graphene, which can be patterned to prepare functional devices for different applications[22]. LDW technique becomes an effective method to produce LIG-materials and has great potential applications in the fabrication and integration of graphene-based devices.

2.2. Immunosensors

Immunosensors are biosensors that use antibodies, antibody fragments or antigens as bioreceptor to monitor specific binding events in biological reactions[27]. These devices have been widely explored in recent years, owing to the need for alternative methods. Due to the specific recognition from the conjugation antigen-antibody, consequently high sensitivity, immunosensors have aroused notable interest for its significant progress in diagnosis and clinical analysis, food safety control, environmental monitoring, public security, etc[49]. Recently, they have exhibited several advantages, including remarkable sensitivity, operational simplicity, low-cost instrumentation, miniaturization, and have provided alternatives for detection of trace amounts of analytical targets, ranging from small molecules (e.g. toxins) and macromolecules (e.g. pathogenic bacteria and viruses)[49]. Thus, they can be used in order to replace conventional methods for foodborne pathogen detection, since they have many advantages that are scarces in existing methods, for example fast response, high sensitivity and selectivity[50]. Furthermore, immunosensors have received particular attention once they can perform direct and label-free measurements, and can be easily manipulated by inexperienced personnel[50].

The use of specific antibodies to detect and to inform certain microorganism or substance is the basic approach utilized in immunosensors. According to Arora et al.[4], antibodies are usually immobilized directly on the electrode surface, and also there are immunosensors based on antibodies immobilized on magnetic beads. The immobilization is mostly made by covalent attaching[6,18,51,52], although there are other techniques such as microcontact printing[53], biotin-streptavidin binding[54–56], direct spotting[54], adsorption to a conductive polymer[57], and so on. The surface-immobilization can cause a considerable loss of biological activity, since the activity of immobilized antibodies depends on their orientation, so assuring that they are not randomly oriented is important[27]. Other reasons for this inactivity include steric hindrance in cases when the density is too high as well as denaturation due to

non-specific interactions with the surface[58], whence the importance of optimizing the amounts of biological material before applying it. An exception to this unwanted loss of activity occurs when impedimetric sensors are used, which will be discussed later. In this case, steric hindrance is promoted due to the interaction between antibody-antigen and reported as a signal.

In assemblies of electrochemical sensors, the transducer must keep a conductive surface even after the immobilization method[18], because the response depends on an electrical signal. In immunosensors, this signal is generated from catalysis promoted by conjugated antibodies that induce some disturbance in the environment, such as ions release, pH change, blocking of electric current flow, oxygen consumption, which are capable to generate an electrical signal on a transducer.

Several approaches were assayed for sensing operations, including antibody-based systems for detection of foodborne pathogens anti-*E. coli* O157:H7 and *Salmonella* spp. [4,6,7,16,52,59,60]. Among other recognition elements, antibodies are most widely used because of their high specificity between antibody-antigen binding, and because they are very sensitive[27].

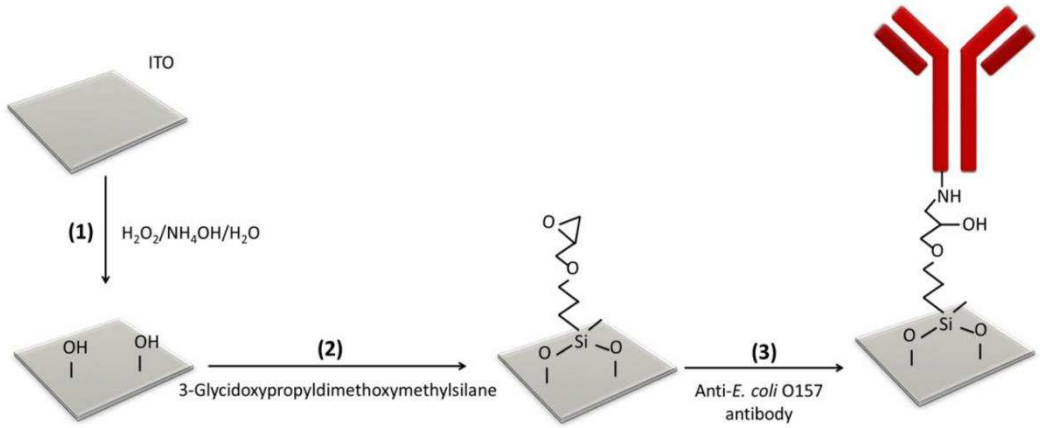

Figure 3. Generic scheme of antibody immobilization on electrode surface. Images obtained and adapted from[6].

2.3. Impedimetric sensors

Impedimetric sensors are non-destructive and potentially sensitive devices that evaluate the impedance from interfacial change without labeling or amplification[61]. Electrochemical impedance spectroscopy (EIS) assays, including faradaic and nonfaradaic measurements,

belong to the main class of impedance spectroscopy (IS), and have been extensively utilized in immunoassays for detection of small target molecules, biomarkers of protein, cells, and pathogens[62]. Taking advantages of label-free, simple, and fast analysis, EIS assays are widely utilized for detection of several biological molecules. For example, Li et al.[63] established a simple immunosensor for testosterone detection by EIS, successfully applied to detect testosterone with a low detection limit of 0.045 ng mL^{-1}. Through functionalization of antibody, Bhardwaj et al.[64] described a conductometric immunosensor of atrazine with high sensitivity and specificity, in a low detection limit of 0.01 nM. To date, EIS technique has also received much attention due to its great possibility to application in detection of pathogenic bacteria. Wan et al.[65] described a signal-off impedimetric immunosensor for detection of *Escherichia coli* O157:H7. The immunosensor was fabricated by covalent immobilization of anti-*Escherichia coli* O157:H7 antibody onto AuNPs and a self-assembled monolayer of a modified gold electrode.

Impedimetric sensors have proved to be a promising method for pathogenic bacteria detection[20] due to their portability, rapidity, sensitivity, low cost, ease of miniaturization, label-free operation, and more importantly, they can be used for direct detection. The impedance (Z), usually expressed as a complex number, is made from the changes that occur in conductance, for example due to bacterial growth, charged ions, compounds resulting from biological metabolism, or due to bacteria adhesion onto the electrode surface[66]. However, impedance is not a selective method. Thus, the selectivity may be achieved by using selective functionalized biomolecules on the electrodes with high-affinity recognition elements, such as antibodies, aptamers, proteins, etc., that selectively bind target molecules permit to considerably enhance the selectivity of the method[66].

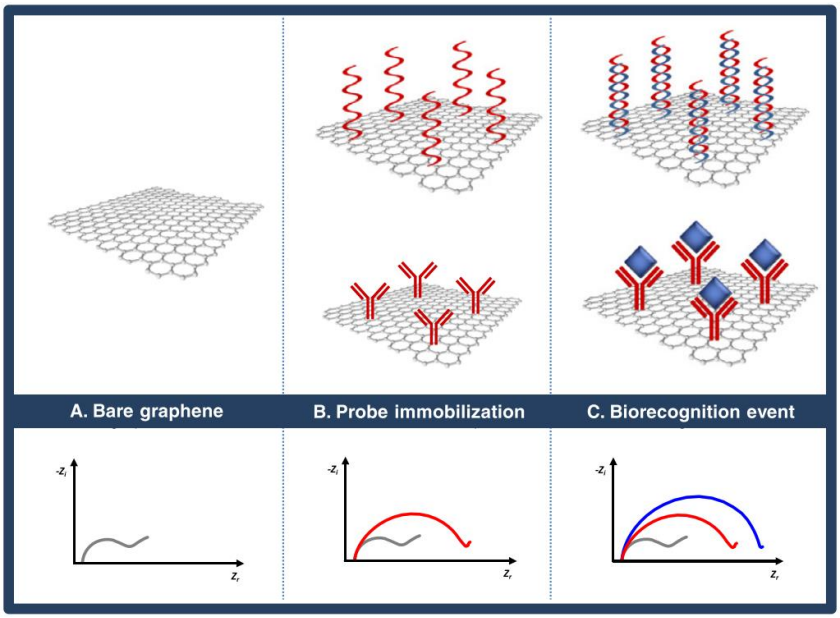

Figure 4. Application of EIS for biosensing detection methods. At the bottom three typical Nyquist Plots are displayed. Images obtained from[62].

The basic principle for understanding the operation of impedimetric sensors is related to changes in the electrical properties at their surface (either capacitance or resistance), affected by interactions between biorecognition element attached to the surface and analyte present in a sample solution[67]. In the present work, the bacteria-antibody interaction hinders the passage of electric current across the electrode surface, which increases the impedance, and consequently implies Nyquist plot curves with larger radius, as shown in Fig. 4. In addition, one of the positive features of the impedance technique is its simplicity. EIS uses a sinusoidal and small-amplitude signal to explore multiple electrical properties of materials[68] and is developing rapidly because fulfills the requirements from conventional sensing methods[69] and can be applied in several areas. Therefore, this technique represents a very powerful tool for investigating the interfacial properties (i.e. resistance and capacitance) of conductive or semi-conductive surfaces. The changes on the electrodes surface are dependent on the biorecognition event, and the measurement does not have any specific pre-treatment[62].

For impedance measurements the transducing material should present a high conductivity and a preferably low electron transfer resistance on its surface[70]. According to Pagliarini et al.[71], label-free assays have aroused interest from scientists for providing fast response measurements and dispensing large amount of reagents and substrates, one of the main

reason why EIS has been widely used. The most frequently used equivalent circuit for modelling data from EIS is the Randles circuit, that consist of electrolyte resistance (R_s), determined by the solution conductivity and the geometry of the surface; charge-transfer resistance (R_{ct}) that reflects the kinetic transfer of charge at the electrode/electrolyte interface; double-layer capacitance (C_{dl}), that represents the electrostatic effect between the electrode and the electrolyte; and Warburg impedance element (Z_W)[67]. This model predicts that the faradaic current resulting from the electronic transfers at the interface is always associated with the capacitive component[72].

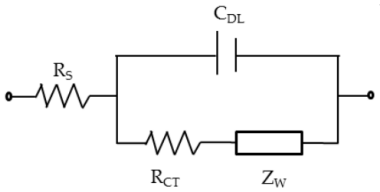

Figure 5. Randles circuit.

A typical shape of the impedance spectrum (Nyquist plot) fitted to this circuit includes a semicircle region observed at high frequency range, that implies a charge-transfer process, and a linear part observed at the low frequency range, that implies a mass-transfer process[73]. The greater the semicircles formed, the greater the charge transfer resistance.

3. Paper

Impedimetric immunosensors based on laser induced graphene to monitor *Salmonella enterica* in food samples

Abstract

Foodborne illnesses are a growing concern for the food industry and consumers, with millions of cases reported every year. Consequently, there is a critical need to develop rapid, sensitive, and inexpensive techniques for pathogen detection in order to mitigate this problem. However, current pathogen detection strategies mainly include time-consuming laboratory methods and highly trained personnel. As an easily obtainable alternative, a recent method to produce graphene, known as laser induced graphene (LIG) is currently being extensively studied due to its facile and inexpensive production and suitability for use in sensing. Herein, we report the fabrication of a highly sensitive and label-free LIG-based impedimetric immunosensor to detect the foodborne pathogen *Salmonella enterica*. Multilayers graphene was produced by laser induction on polyimide film and confirmed by Raman spectroscopy. The electrochemical performance of the electrodes was verified by cyclic voltammetry (CV) and electrochemical impedance spectroscopy (EIS), conferring similar or even better characteristics than existing studies displaying a charge transfer resistance of 577 ± 48 Ω with an electroactive surface area of 0.104 ± 0.032 cm^2. *Salmonella*-antibodies were immobilized onto LIG electrodes to produce the immunosensors. After functionalization, the detection ability was evaluated by EIS. The calibration curve showed a large linear range from 10^1 to 10^5 CFU mL^{-1} and a sensitive limit of detection of approximately 13 ± 7 CFU mL^{-1} in chicken broth, with a response time of 22 minutes. The immunosensors displayed high selectivity as demonstrated by no detection of non-specific bacteria *Escherichia coli*, with less than 2% change in signal-to-noise ratio over 10^2 to 10^7 CFU mL^{-1} of *E. coli*. The results show one of several possible applications of LIG-based electrochemical sensors for bacteria detection as impedimetric immunosensors, highlighting its low-cost, easy fabrication, sensitivity, easy operation, and no requirement of sample preparation. Hence, the developed biosensor is well-suited for in-field use such as food processing facilities.

Keywords: *Salmonella enterica*; Laser induced graphene; Electrochemical Impedance Spectroscopy; Food safety; Disposable sensor.

3.1. Introduction

Nearly half a million people die each year from acquiring foodborne illness[1]. With the sharp increase in population, over 9 billion by 2050 according to the United Nations (UN) prediction[74], the demand for food production has grown substantially, requiring an efficient food quality control proportional to growth to avoid foodborne diseases and contamination. According to the United States Department of Agriculture (USDA), non-typhoidal *Salmonella* causes an estimated $3.7 billion in economic burdens each year, and is the leading cause in hospitalization and deaths due to foodborne illnesses with exposure occurring through food, water, and contaminated surfaces[75]. Despite strict regulations to control the presence of *Salmonella* in food supply, there is an increasing incidence of illness from foodborne contamination[8], probably due to inefficient methods used by food industries for safety control that are oftentimes time consuming, far from the production line, and sometimes do not point out the necessary sensitivity. Therefore, studies are necessary to enable the implementation of simple, rapid, inexpensive, and reliable food safety control methods, preferably with portable sensor systems[10], that can be used on-site.

Recent studies reported label-free methods of highly sensitive and very accurate *Salmonella* detection; however, oftentimes these devices require expensive materials, complex construction, sophisticated equipment, difficult production on a large scale, and are time-consuming[17,18,76]. Biosensors are devices that have been explored extensively in recent years as an alternative to conventional methods for detection of pathogenic bacteria, mainly due to their high specificity, excellent sensitivity, and fast response time[2,4]. They have received particular attention since they can perform direct and label-free measurements, and can be easily manipulated by personnel without previous training[6,71,77]. Studies involving graphene and carbon nanotubes applied to food safety and sustainable agriculture have increased in recent years[77].

Within the category of two dimension crystals, graphene is an outstanding material due to its structure and exceptional properties[21,78]. Graphene is a sheet of sp^2 bonded carbon atoms arranged into a rigid hexagonal lattice, exhibiting a set of properties that no material has concomitantly displayed; among them, high mechanical strength (1 Tpa), excellent electrical conductivity and charge carrier mobility (~10^5 cm^2/Vs), large specific surface area (~2630 m^2/g), and high impermeability and biocompatibility[19,24,79]. In addition, due to the advantages of its morphology and its properties, graphene-like nanomaterials have attracted attention as

emerging materials for electrochemical sensor applications[80]. Hence, techniques for graphene synthesis have grown considerably to supply the demand for this material[78], however, common methods of synthesis, such as mask lithography[36,37], inkjet direct-printed[30], and LightScribe DVD optical drive[81] include either high thermal requirements or multiple steps towards chemical formation of graphene[33].

An alternative to expensive techniques is to produce sensors based on graphene through screen printing, or more recently inkjet printing[30,82,83]. These methods have been highly studied, but often require post-print annealing processes to increase the electrical conductivity of the printed graphene and many treatment steps[11]. As an alternative to these techniques, the Tour group[12] introduced a simple method dubbed laser induced graphene (LIG) which is a "direct-write" method that can be used in a one-step process to convert carbon sp^3 into carbon sp^2 under high temperature promoted by laser induction, which confers porous graphene[15]. Because it can be obtainable from commercial polymers, with an easy manufacturing process, LIG has been applied towards stretchable and sensitive strain gauges[84], microsupercapcitors[85], UV photodetectors[86], sound generators and detectors[87], and electrochemical sensors[25]. Currently many studies have addressed electrochemical sensors for broad detection, whether in the environmental, medical or food sector.

Herein, we report on the first LIG sensor that is capable of rapid and quantifiable detection of *Salmonella enterica* concentrations in food samples. Porous graphene was produced from polyimide by laser induction, and the materials were characterized conferring a new potential application in the sensing field. An impedimetric immunosensor was developed based on LIG-electrodes functionalized with specific antibody for detection of *Salmonella enterica*, one of the most prominent foodborne pathogens[7]. The immunosensor was able to detect the pathogen at low concentration, 13 ± 7 CFU mL^{-1} in complex media, chicken broth with a response time of around 20 minutes. Electrochemical impedance spectroscopy was used as a label-free detection over a broad range of bacteria concentration, from 10^1 to 10^5 CFU mL^{-1}. Moreover this promising device is a low cost and disposable sensor that can be used in-field such as food processing facility, assisting in containing contamination before it spreads, which reinforce its important contribution to food safety.

3.2. Material and Methodes

3.2.1. Materials

Kapton® (polyimide) tape 0.07 mm was purchased from McMaster-Carr co. (USA), and Epson Ultra Premium Photo Luster 240 g m^{-2} from Office Depot (USA). Potassium Ferro/Ferricyanide, N-hidroxissuccinimida (NHS), 1-Ethyl-3-(3-dimethylaminopropyl) carbodiimide (EDC), 2-(N-morpholino) ethanesulfonic acid (MES) and ethanolamine were purchased from Sigma-Aldrich (USA). Potassium chloride and SuperBlock™ in phosphate buffered saline (PBS) (used as blocking buffer) were purchased from ThermoFisher Scientific (USA). KPL BacTrace® polyclonal andibody anti-*Salmonella* was purchased from SeraCare (USA). PBS was purchased from Aplha Aesar (USA) and Chef's Cupboard Chicken Broth was purchased from local supermarket. All the chemicals used in the study were analytical grade. Solutions were made using deionized water generated by a Milli-Q water purification system (Millipore, USA), with an electric resistance ≈18.2 MΩ.

3.2.2. Laser induced graphene electrode fabrication

The working electrode was designed using a linear sketch pattern (0.17 mm separation) in SolidWorks 2018 (Dassault Systems, France), and the engraving process was performed with a 75W Epilog Fusion M2 CO_2 laser (Epilog Laser, USA) at 7% speed and 4% power with a lens to material distance of ~74 mm and beam size of ~176 μm in ambient atmosphere. The laser induction was carried out on polyimide film taped onto the emulsion side of the photo paper, according to Tehrani and Bavarian[26], and Fenzl et al.[88]. This procedure produced LIG-electrodes as shown in Figure 6. The working area (3-mm diameter) and connector ends of the working electrode were separated by a layer of fast drying nitrocellulose lacquer (passivation layer) used to cover the non-active areas of the electrodes.

3.2.3. Material characterization

The Raman spectrum was obtained by using a Renishaw InVia confocal Raman microscope with a 633-nm laser source (0.12 mW), a 50x objective lens and a diffraction grating of 1800 lines, in order to confirm the graphene formation by the laser induction process. The crystallinity of the bare electrodes and the level of graphitization were evaluated using a Bruker D8 DISCOVER X-ray Diffractometer provided with copper radiation (λ = 1.542 Å) scaning θ/2θ. A scanning electron microscope JEOL JSM-6010LA equipped with an energy

dispersive spectroscopy (EDS) system was used to obtain images of the LIG morphology at 230x, 2000x, and 2300x magnififcation and the electrode's chemical composition, at accelerating voltage of 5 kV.

3.2.4 Antibody functionalization onto LIG-electrodes

The working area of the electrodes were covered with 30 µL of EDC/NHS (3:1) solubilized in sterile filtered MES (pH 6.0) for 1 hour and then rinsed with PBS buffer to remove the excess EDC/NHS. Next, 1 µM previously optimized of polyclonal antibody anti-*Salmonella* was applied to the surface of the working electrode followed by overnight incubation at 4 °C. The electrode was then rinsed with PBS buffer, dried at room temperature, and afterwards, 1 M ethanolamine was applied for 20 minutes to quench the remaining unreacted EDC/NHS. The unreacted graphitic surface was blocked using Superblock® in PBS, for 20 minutes, to reduce non-specific binding, and then rinsed off with a 1x dilution of PBS (1x PBS) pH 7.4, prior to testing.

3.2.5. Electrochemical characterization

The electrochemical proprieties of the LIG-electrodes were analyzed using cyclic voltammetry (CV) and electrochemical impedance spectroscopy (EIS). All electrochemical measurements were carried out on a CH Instruments Electrochemical Analyser (CHI7081E model) at room temperature. The 3-electrode system consisted of a CH Instruments Ag/AgCl reference electrode and platinum counter electrode with the LIG functioning as the working electrode. CV and EIS experiments were carried out in 10 mL solution containing 0.1 M KCl, 4 mM $K_3[Fe(CN)_6]$ and 4 mM $K_4[Fe(CN)_6]$ (1:1). The scan rates used for CV measurements were 50; 75; 100; 125; 150; 175; 200 mVs^{-1}, in a sweep range from -0.4 V to 0.6 V, and quiet time of 2 seconds. EIS analyses were performed in the frequency range of 1 MHz – 100 Hz, using AC amplitude of 10 mV and DC voltage of 0 V.

3.2.6. Bacteria sample preparation

Salmonella enterica subsp. enterica serovar Typhimurium (ATCC 14028) and *Escherichia coli* O157:H7 (ATCC 43895) were resuscitated through 2 consecutive 24 h growth cycles in TSB at 35 ºC to obtain working cultures containing approximately 10^9 CFU mL^{-1}. Bacteria cultures were renewed weekly in TSB (i.e., one transfer followed by 24 h incubation

in aerobic conditions) and maintained at 4 ºC. Samples of bacteria were serially diluted in BPW, plated via spread plating on TSA and incubated for 18 hours at 35 °C before counting the colony growth, and results were reported as CFU mL^{-1}. Different bacteria concentrations were prepared in 15 mL of BPW or chicken broth in order to validate the impedimetric immunosensor and to simulate its application in food. These concentrations were confirmed by plate counting. Both bacteria concentrations ranged from approximately 25 to 10^5 CFU mL^{-1}.

3.2.7. Bacteria sensing

The presence of bacteria was evaluated by EIS analysis, measuring different bacteria concentrations directly in suspension with incubation time of 20 minutes under 100 rpm and analysis time of 90 seconds. Before testing the immunosensor in complex media, its performance was verified in pristine buffer, BPW. The LIG based immunosensor was also subjected to selectivity testing with a negative control, *E. coli* O157:H7, also Gram-negative as *Salmonella* and a pathogen of major concern, under the same conditions as those used for *S. enterica*. Between each measurement, the electrode was thoroughly washed with PBS to remove unbound bacteria. Complex plane diagrams (Nyquist plots) were used to determine the charge transfer resisitance (R_{ct}), the solution resistance (R_s), the double-layer capacitance (C_{dl}), and the Warburg element (Z_W)[89], fitting the EIS data sets to an equivalent cirucuit model (i.e., Randles circuit) through EIS Spectrum Analyser from http://www.abc.chemistry.bsu.by/vi/analyser/.

3.2.8. Data Analysis

All measurements were made in triplicate and results were expressed as mean ± standard deviation. Differences between variables were tested for significance using one-way analysis of variance (ANOVA) and significantly different means ($p < 0.05$) were designated using Tukey's Honestly Significant Differences (HSD) test through JMP v.13 Software (SAS Institute, USA). The functional correspondence among quantitative variables was performed using SigmaPlot 12 by regression analysis. To evaluate the electroactive surface area (ESA) and the constant for heterogeneous electron transfer rate (k^0), the peak current values and peak potential separation from the CV results were used to solve the Randles-Sevick equation as previous works[25,50] and to apply the Nicholson method for reversible electron tranfers[90], respectively. The 3σ method was used to calculate the limit of detection (LOD) and

sensivity[50,91]. Please, see Appendix for further details on calculations and data presentation and analysis.

3.3. Results and Discussion

3.3.1. LIG-electrodes characterization

SEM was used to characterize the surface topography of the LIG electrodes (Fig. 7 A-C). A carbon structure in hexagonal-planar configuration was formed, as well as a highly porous 3D electrode rich in edge-planes pyrolytic graphite (EPPG) (Fig. 7B). The cross-sectional image (Fig. 7C) shows the LIG-electrode as a macroporous/mesoporous structure with a thickness of 15-20 µm. The irradiation from this laser produced porous graphene onto polyimide film by converting the carbon from polyimide into graphitic carbon[12]. The lasing process converts the sp^3 carbon into sp^2 by photothermal effects, due to the high temperatures reached at the surface (> 2500 ºC)[12,24]. As demonstrated in Fig. 7 A-C, this ablation procedure is able to provide a carbon frame organized into long-range ordered graphene layers[28]. According to Nayak et al.[25], the available edge-plane sites formed on the surface of the LIG-electrodes contribute to the electron transfer. The 3D morphology confers higher and more accessible electrochemical surface area, allowing electrolyte penetration more easily into the active area.

To anlalyze the structure of the materials as well as the surface molecular groups, the electrodes were evaluated with Energy Dispersive Spectroscopy, Raman spectroscopy, and X-Ray Diffraction (XRD). The C—O, C—N and C=O bonds originally present in polyimide film could easily be broken by the high temperature[12], as confirmed by EDS. Assuming $(C_{22}O_5N_2H_{10})_n$ as the polymer chain from Kapton® tape, the initial composition could be calculated to 69.1%, 21.0%, 7.3% and 2.6% m/m for C, O, N and H respectively, which was converted to 97.5% C and 2.5% O after lasing, with N, H and O being released as gases due to the strong heating[24].

Raman spectroscopy was used to characterize the graphitic material according to its crystalline quality, observed from sharp peaks[92]. This technique is also useful to characterize disorder in the sp^2 carbon lattice[24]. The Raman spectrum showed three main peaks displayed in Figure 7F. The first order D peak (roughly at 1350 cm^{-1}) indicates lattice defects caused by bents in the sigma bonds; the first order G peak (roughly at 1580 cm^{-1}) shows the lattice vibrations of the sp^2 carbon atoms; while the second order 2D peak (roughly at 2660 cm^{-1})

shows a distinctive peak of graphene structure[26,93]. The ratio I_{2D}/I_G refers to the number of graphene layers, and according to the obtained ratio $I_{2D}/I_G \sim 0.35$ multilayer graphene was formed[92,94]. As expected, these peaks were not observed on original polyimide film (Fig. 7F). A complementary analysis of LIG-electrodes by X-Ray Diffraction (XRD), displayed a peak located at $2\theta = 26.5°$ (Fig. 2E). A very similar result was reported by Nayak et al.[25] at $2\theta = 26.4°$, and also a peak at $2\theta = 25.9°$ was reported by Chen et al.[13], Lin et al.[33], and Zhang et al.[28], indicating the presence of C (002) peak, with an interlayer spacing (I_c) of ~3.36 Å between LIG-planes, which indicates a high degree of graphitization[12].

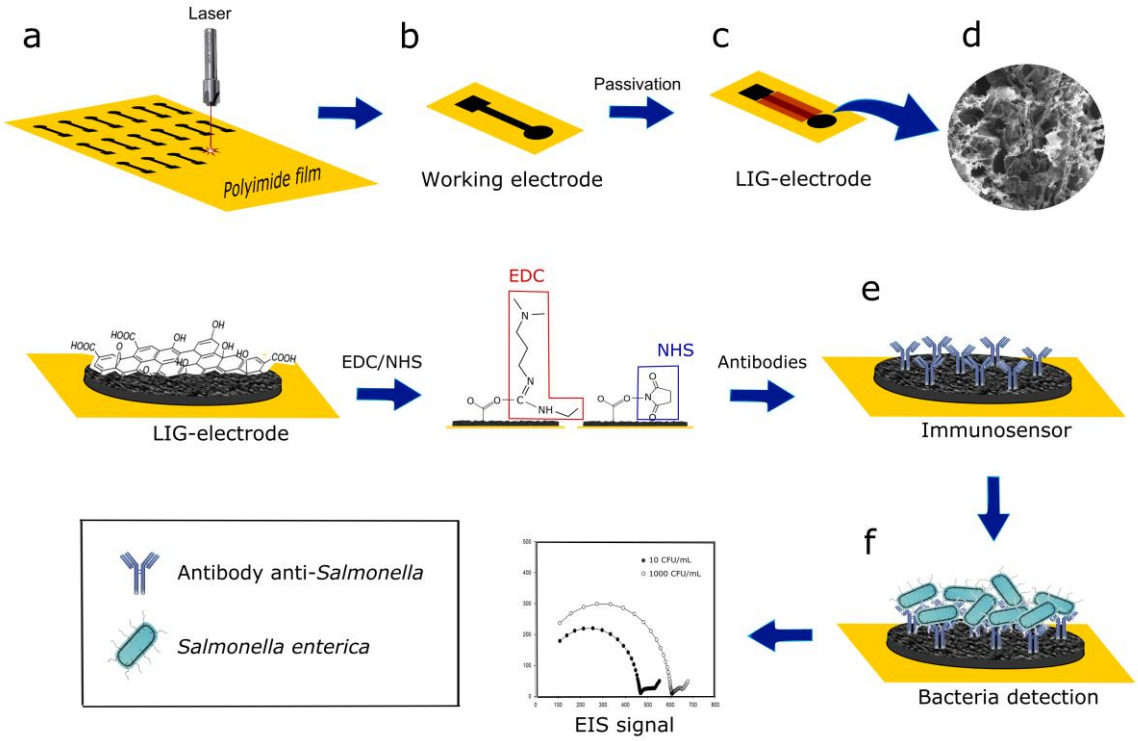

Figure 6. Fabrication, biofunctionalization, and sensing scheme of LIG immunosensor. Fabrication and biofunctionalization steps included (a) LIG processing onto a polyimide (Kapton®) sheet to create (b) working electrode, (c) passivation of working electrode with nitrocellulose lacquer, (d) SEM image showing LIG surface, (e) biofunctionalization with *Salmonella* antibodies immobilized on the working electrode via carboiimide cross-linking chemistry, and (f) *Salmonella* binding to the electrode and the resultant Nyquist plot generated during electrochemical sensing.

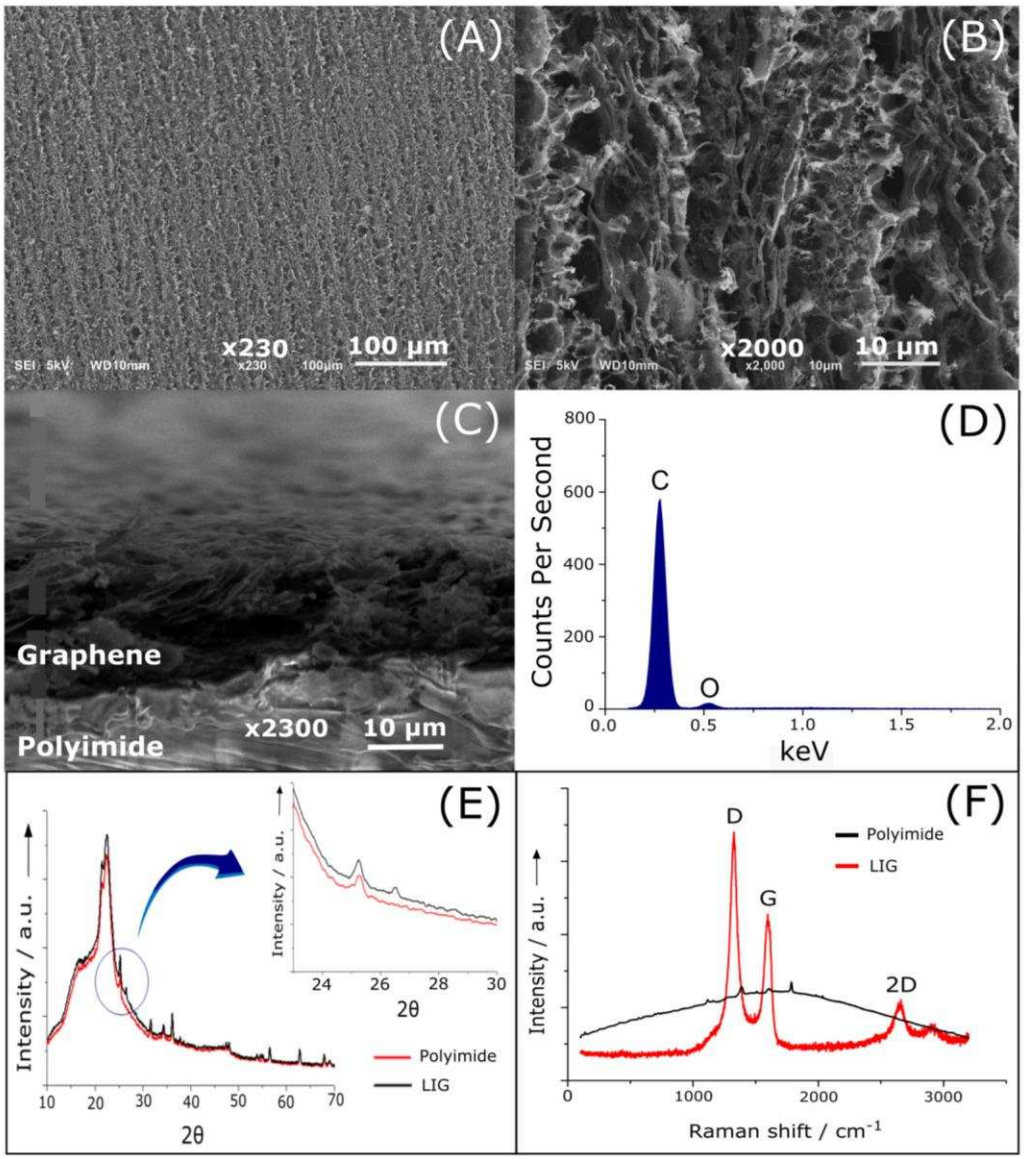

Figure 7. (A, B) SEM images of the bare electrode at 5 kV and 230-2300X magnification, confirming the porous graphene morphology; (C) Cross-sectional image of the same electrode; (D) EDS spectrum of the LIG-electrode, showing the predominance of carbon and a small portion of oxygen, responsible for promoting the covalent bonds; (E) Representative XRD spectrum comparing PI and LIG which displays a peak at 26.5º indicating graphitization; (F) Raman spectrum also comparing PI and LIG showing the three characteristic peaks for graphene material D, G and 2D which indicates multi-layer graphene formation.

3.3.2. Electrochemical characterization

The electrochemical performance of the bare LIG-electrodes was investigated in order to verify its ability to act as electrochemical transducer. CV curves were recorded and for all scan rates tested, the electrodes displayed well-defined redox peaks (Fig. 8A-B), disclosing its quasi-reversible behavior[90]. The small change in peak separation (ΔE_p) observed from these curves indicated a fast electron transfer rate, which is related to the reversibility of electron transfer, and derived from the presence of EPPG, caused by the high incidence of defects[25], previously shown by the Raman spectrum (Fig. 7F). The electroactive surface area (ESA = 0.104 ± 0.032 cm^2) was approximately 50% higher than the geometric area (0.071 cm^2), similar to that found by Nayak et al.[25], who reported ESA = 0.092 ± 0.015 cm^2 for the same geometric area. This is likely due to the porous graphene structure that increases the surface area[88].

The CV curves also confer information about the heterogeneous electron transfer rate (HET) between the electrode and the redox mediator species[25]. The HET constant obtained (k^0 = 0.0146 ± 0.0031 cm·s^{-1}) exceeds those found by other groups[50,59,88] ranging from 0.0030 to 0.0044 cm·s^{-1} for LIG with the same redox ferro/ferriciyanide species. It also exceeds commercial edge plane pyrolytic graphite (0.0026 cm.s^{-1}) and basal plane pyrolytic graphite (0.0003 cm.s^{-1}) as reported in a previous study by Griffiths et al.[95]. These results confirm the effective electron transfer kinetics of LIG produced in this study, and its feasibility to use as an electrochemical transducer.

EIS measurements are an efficient method to probe the interfacial characterization of the electrode[96,97]. The diameter of the semicircle is a measure of the charge transfer resistance (R_{ct}) and was used to characterize the bare LIG-electrodes (Fig. 8C). The reported $R_{ct} = 577 \pm 48$ Ω was substantially lower when compared with others carbon surfaces, as glassy carbon[98] and graphite electrodes[62,99] with values around 2 and 7 kΩ, respectively. Therefore the results obtained from CV and EIS confirm that the LIG-electrode is suitable for electrochemcial sensing.

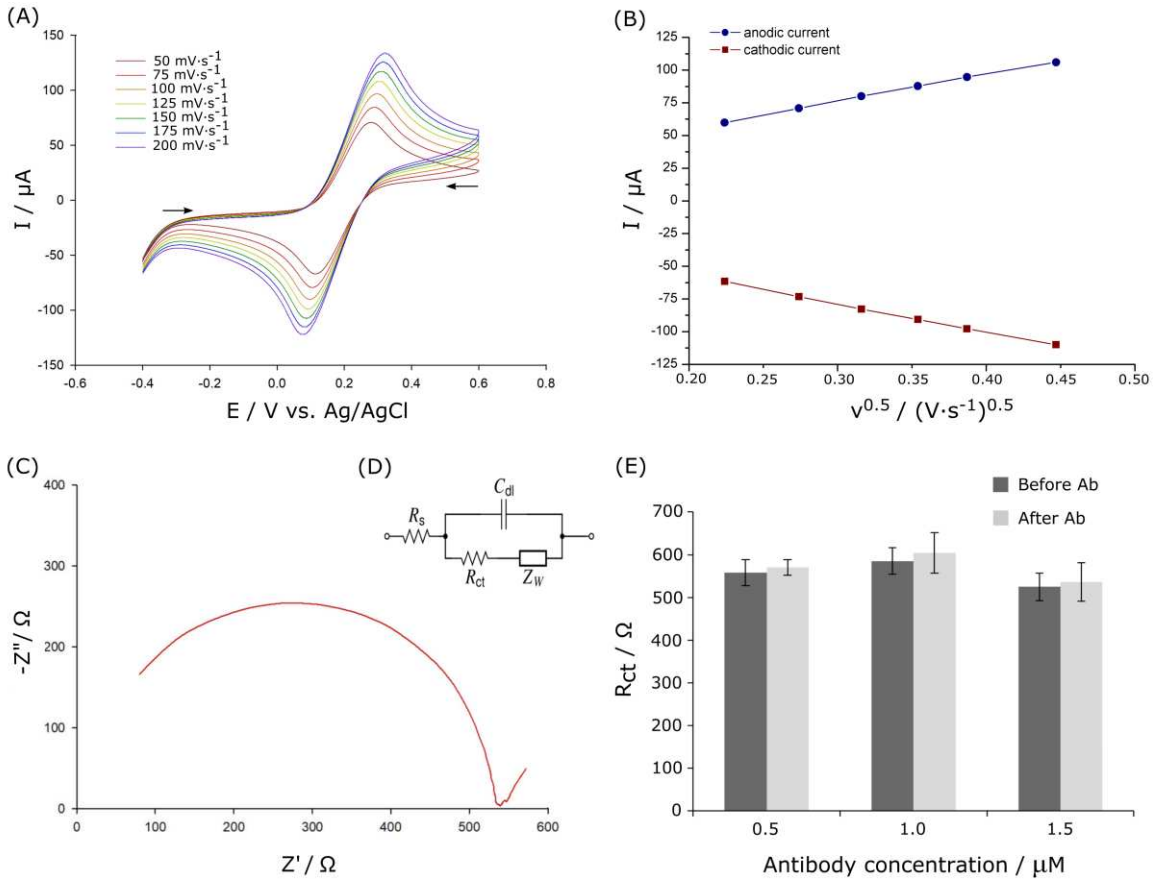

Figure 8. (A) Representative cyclic voltammogram of LIG-electrode vs. Ag/AgCl in 0.1 M KCl containing 4 mM $K_3[Fe(CN)_6]/K_4[Fe(CN)_6]$ at scan rates from 50 to 200 $mV \cdot s^{-1}$; (B) Cottrell plot of LIG-electrode vs. Ag/AgCl in the same solution at scan rates 50, 75, 100, 125, 150 and 200 $mV \cdot s^{-1}$ with corresponding values of ESA = 0.104 ± 0.032 cm^2 and k_0 = 0.0146 ± 0.0031 cm s^{-1}; (C) Nyquist plot confirming $R_{ct} \approx 550\ \Omega$ for the LIG-electrode; (D) Equivalent Randles circuit used to fit the curves and to calculate the R_{ct}; (E) Optimization of antibody concentration showing no significant difference to R_{ct} variation according to Tukey-HSD test ($p < 0.05$).

3.3.3. Immunosensor performance

The bare LIG-electrode was converted into an immunosensor by functionalizing the surface with specific polyconal antibodies to detect *Salmonella enterica* via carbodiimide cross-linking (see methods), as shown in Figure 6. In order to define the optimum loading concentration of antibody on the working electrode, three different concentrations, 0.5, 1.0 and 1.5 µM, were tested by measuring the change in charge transfer resistance (ΔR_{ct}). Results

showed no significant difference among these concentrations at $p < 0.05$, with ΔR_{ct} ranging around 1-2 % (Fig. 8D). Therefore, 1.0 μM was chosen since it is an intermediate value and already used in previous studies[100]. The immunosensor was initially tested in bufferd peptone water (BPW) in order to verify its sensing performance in simple media, and then it was tested in chicken broth to simulate real food samples. *Salmonella enterica* detection was evaluated with EIS, and the change in R_{ct} from the suspension to the electrode was used to produce the calibration curve. Change in the R_{ct} is proportional to the adhesion of bacterial cells to the biofunctionalized region of the electrode[6]. This "bio-barrier" hinders the electrolyte access, acting as a blocker, increasing the R_{ct}[69,101,102]. According to this technique a larger radius corresponds to a larger R_{ct}, which represents a greater accumulation of bacteria caused by the specific interaction with antibodies on the surface of the electrode[6]. Figure 9 displays the Nyquist plot, a typical impedance spectrum, which shows the increase in R_{ct} with increasing *Salmonella enterica* concentration, obtained from testing the immunosensor in both suspensions, BPW and chicken broth (Fig. 9A and 9C, respectively). A linear increase in the $\%\Delta R_{ct}$ as a function of bacteria concentration is also shown for BPW and chicken broth (Fig. 9B and 9D, respectively).

The presence of attached bacteria cells plays the role of electron kinetic barrier as well as steric hinderance[102], decreasing the electron transfer path between the electrolyte solution and the electrode, and consequently resulting in the increase of R_{ct} values. A calibration plot was obtained by normalizing the R_{ct} with respect to the R_{ct} value measured for zero concentration of *Salmonella enterica* in the buffer solution. The LIG-based immunosensor presented a linear sensing range from 10^1 to 10^3 ($R^2 = 0.984$), with a sensitivity of 42 Ω/log CFU mL^{-1} and a limit of detection of 10 CFU mL^{-1} in buffer (Fig. 4A-B). To prove potential of the LIG-based immunosensor in the evaluation of real food samples, chicken broth was used as the sensing matrix. Similarly, a calibration plot was obtained by normalizing R_{ct} values with plain chicken broth. Based on the calibration plot, the linear sensing range for *Salmonella enterica* detection in chicken broth was between 10^1 and 10^5 ($R^2 = 0.989$) with a sensitivity of 24 Ω/log CFU mL^{-1} and a limit of detection of 13 CFU mL^{-1} (Fig. 9C-D). The total response time for all immunosensing tests was 21.5 minutes, which consisted of 20 min to allow bacteria contact with the LIG electrode and 90 s to collect EIS measurements.

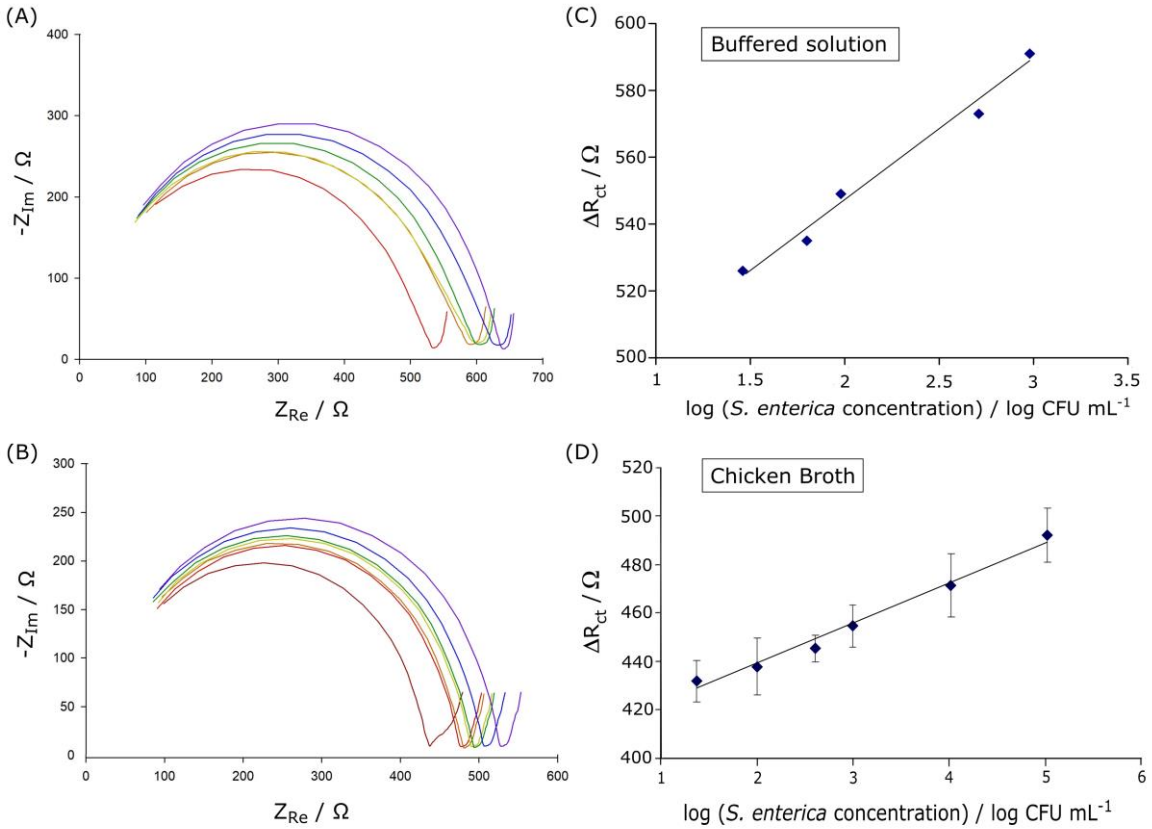

Figure 9. Representative Nyquist plots of impedance spectra of the immunosensor for increasing concentration of *Salmonella enterica* at: (A) 0 CFU·mL^{-1} (red), 29 CFU·mL^{-1} (orange), 63 CFU·mL^{-1} (yellow), 96 CFU·mL^{-1} (green), 512 CFU·mL^{-1} (blue), and 957 CFU·mL^{-1} (purple) in BPW; (B) 0 CFU·mL^{-1} (brown), 33 CFU·mL^{-1} (red), 92 CFU·mL^{-1} (orange), 444 CFU·mL^{-1} (yellow), 923 CFU·mL^{-1} (green), 10^4 CFU·mL^{-1} (blue), and 10^5 CFU·mL^{-1} (purple) in chicken broth; bacteria concentrations were confirmed by plate counting; (C-D) Linear calibration curve of charge transfer resistance change (ΔRct) versus *Salmonella enterica* concentrations (log CFU·mL^{-1}) in (C) BPW showing a linear regression corresponding to ΔRct = 41.9 log (concentration of bacteria) + 463.2 with R^2= 0.984 and (D) in chicken broth with a linear regression corresponding to ΔRct = 16.7 log (concentration of bacteria) + 402.4 with R^2= 0.989; data shown as mean ± SD, n= 3. Plots were generated from graphs (A) and (B).

The LIG based immunosensor was also subjected to selectivity testing with a negative control, *Escherichia coli*, under the same conditions as those used for *Salmonella enterica* in chicken broth. The R_{ct} values recorded from *E. coli* sensing did not show significant change with the increase of bacteria concentration (Fig. 10A), with less than 2% change in signal-to-

noise ratio over 10^2 to 10^7 CFU mL^{-1} of *E. coli* (Fig. 10B). In contrast, the signal-to-noise ratio strongly is pronounced in the presence of *Salmonella enterica* as it can be seen with the addition of 33 CFU mL^{-1} *Salmonella enterica*.

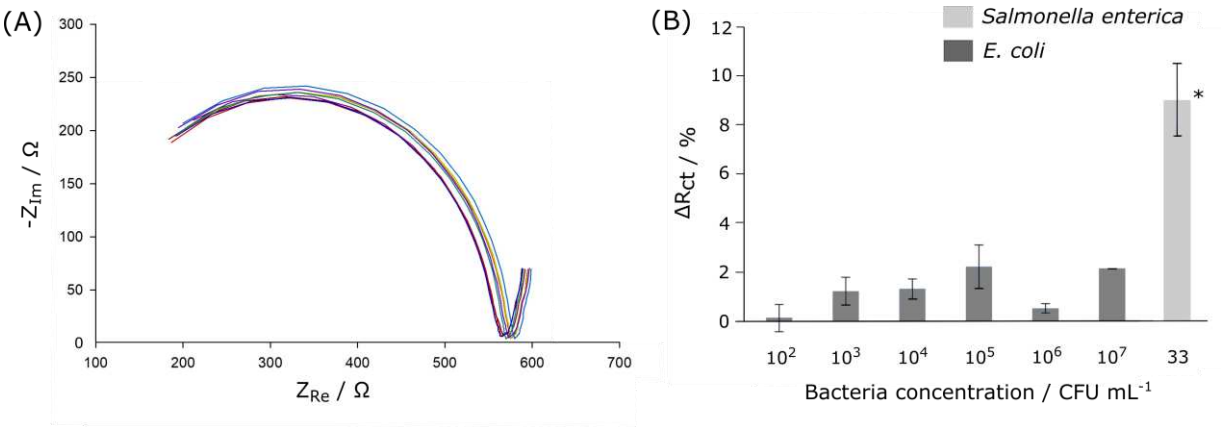

Figure 10. (A) Representative Nyquist plots of impedance spectra using a non-specific pathogen *Escherichia coli* O157:H7 in chicken broth to demonstrate immunosensor selectivity. (B) Percentage charge transfer resistance change (ΔRct%) versus bacteria concentrations (CFU·mL^{-1}) to show specificity of the immunosensor between the target bacteria *Salmonella enterica* and negative control *E. coli*, which is demonstrated by less than 2% change in ΔR_{ct} over 10^2 to 10^7 CFU mL^{-1} of *E. coli* compared to *Salmonella enterica* with ΔR_{ct} starting at around 10% for a concentration of 33 CFU mL^{-1}, n= 3. Plot B was generated from graph A. Bacteria concentrations were confirmed by plate counting.

The developed immunosensor exhibited overall good performance using easily obtainable and inexpensive materials with a cost estimate of $2 per immunosensor, which contributes to its accessible fabrication. Previous studies have elaborated highly sensitive and label-free sensors, for example those based on ion selective electrodes made of gold nanoparticles[17] and double-walled electrode made of carbon nanotubes[76], but all required time greater than 20 minutes, as reported here (see comparsion on Table 1). In addition, much has been advanced in the field of biosensors for pathogens detection, but according to the information from this table, biosensors that display performance similar to this work use expensive or complex materials, such as gold nanoparticles. Such comparisons indicate that there are no records of a fast, sensitive and simple device like the one demonstrated in this work.

Table 1. Comparison among different electrochemical biosensors for *Salmonella* spp. detection.

Transducer	Material	Detection Technique	LOD (CFU mL^{-1})	Working range (CFU mL^{-1})	Analysis time	Sample	Ref.
GCE	rGO	DPV	10^1	10^1-10^8	1 h	Chicken in BPW	[89]
ISE	AuNPs	P	6	10^1-10^6	1 h	PBS, Apple juice	[17]
SPE	rGO	EIS	10^1	-	-	Water and Juice samples	[102]
SP-IDME	Gold	EIS	10^3	10^3-10^6	< 2 h	Chicken rinse water	[16]
SPE	Gold	EIS	-	10^3-10^7	90 min	Redox solution	[71]
SPE	Gold	EIS	10^3	10^3-10^8	20 min	PBS, Milk	[103]
SPE	Gold	CA	21	10^1-10^7	-	Chicken in liquid samples	[104]
DWE	CNTs	CA	9	10^2-10^7	6 h	PBS	[76]
IME	Gold/MSNTs	I	500	10^3-10^7	30 min	PBS	[60]
SPE	Gold	CA	10	10^1-10^5	125 min	Milk	[18]
LIG	Multilayers Graphene	EIS	10	10^1-10^3	22 min	BPW	This work
LIG	Multilayers Graphene	EIS	13	10^1-10^5	22 min	Chicken Broth	This work

Glassy Carbon Electrodes (GCE), Ion Selective Electrodes (ISE), Screen-Printed Electrodes (SPE), Interdigitated Microelectrode (SP-IDME), Double-Walled Electrode (DWE), Interdigitated Microelectrode (IME), Reduced Graphene Oxide (rGO), Gold Nanoparticles (AuNPs), Carbon Nanotubes (CNTs), Magnetic Silica Nanotubes (MSNTs), Buffered Peptone Water (BPW), Differential Pulse Voltammetry (DPV), Potentiometry (P), Chronoamperometry (CA), Impedimetry (I).

3.4. Conclusions

This work reports on a highly sensitive, selective and simply fabricated impedimetric immunosensor by direct formation of graphene on commercial polyimide film through a laser induction technique. The results obtained reinforce that this sensor can be implemented worldwide due to its easy fabrication and accessibility, which has great potential for food safety monitoring. It is a versatile device that can be elaborated for monitoring other pathogens, depending only on the selectivity of the bioreceptor. The working electrode based on LIG presented excellent electrochemical performance and were functionalized with antibodies for *Salmonella enterica* detection, since there are no previously reported studies using LIG-eletrodes to monitor this pathogen. The immunosensor was able to detect the target bacteria at a low concentration of 13 ± 7 CFU mL^{-1} in complex media such as chicken broth in just 20 minutes without addition of exogenous reagents, which corresponds to response time and detection limit that has been never previously reported. In addition, the sensor showed a wide linear range, from 10^1 to 10^5 CFU mL^{-1}. Therefore, impedimetric immunosensors based on LIG are very promising for bacteria sensing, since it is easily manufactured in ambient conditions compared to other complex fabrication procedures that require CVD[92] and/or complex substrate-transfer techniques, ink and ink-preparation[30] or post-printing processes[11]. Consequently, resulting in a low-cost fabrication process that produces porous graphene with high electrical conductivity, and good chemical stability[22]. All these properties promise to make this sensor an extremely viable device to be used for food safety monitoring and an excellent platform for future electrochemical sensors.

4. Final considerations

It is known that the exceptional properties of graphene make it feasible for several electrochemical biosensor applications. However, some limitations concerning its synthesis methods hampered its expansion, but numerous efforts have been established to solve these obstacles. Thus, this novel technique LIG provides consistent graphene production with defined properties in a large scale and cost-effectively, indispensable for future commercialization.

There are many methods for immobilizing biological materials such as chemical adsorption, covalent immobilization, encapsulation, among others. In this work antibodies were immobilized onto LIG-electrodes by covalent functionalization through the cross-linker solution EDC / NHS. Although it is an efficient and very used mechanism, its optimization was not tested. It would be interesting to test it in future research projects to optimize the amount of antibodies and reagents expended and to check if they will be properly immobilized, in order to develop a highly effective and reproducible immunosensor.

In spite of extensive studies that have been made to fabricate novel electrochemical biosensors, long-term stability and application in real sample matrices should be considered. In this case it was possible to obtain good results testing the developed device in complex media such as chicken broth, since real biological fluids contain molecules and ions which undermine the performance of electrochemical biosensors.

In further experiments it would be interesting to test the sensor in solid food samples. In addition, a suggestion for upcoming studies is to evaluate the durability of the developed immunosensor over time, in order to verify its kinetic stability. Another important point to take into account is the demand on developing new methods for pathogen detection that distinguish viable cells from non-viable ones. Furthermore, it would be interesting to test several negative controls and the target pathogen in the same solution to test accurately their selective performance.

In this work we presented the results from a developed impedimetric immunosensor, which will lead to a significant advance in analytical applications for the highly effective and sensitive detection of *Salmonella* and open new paths in several fields.

References

1. WHO-2015. Who Executive Summary of Food Borne Diseases -2016. *Who Exec. Summ. Food Borne Dis. -2016* 1–2 (2015).
2. Lazcka, O., Campo, F. J. Del & Muñoz, F. X. Pathogen detection: A perspective of traditional methods and biosensors. *Biosens. Bioelectron.* **22,** 1205–1217 (2007).
3. Vanegas, D. C. & Gomes, C. Biosensors for Indirect Monitoring of Foodborne Bacteria. *Biosens. J.* **5,** 1–3 (2016).
4. Arora, P., Sindhu, A., Dilbaghi, N. & Chaudhury, A. Biosensors as innovative tools for the detection of food borne pathogens. *Biosens. Bioelectron.* **28,** 1–12 (2011).
5. Guan, J.-G., Miao, Y.-Q. & Zhang, Q.-J. Impedimetric biosensors. *J. Biosci. Bioeng.* **97,** 219–226 (2004).
6. Barreiros dos Santos, M. *et al.* Label-free ITO-based immunosensor for the detection of very low concentrations of pathogenic bacteria. *Bioelectrochemistry* **101,** 146–152 (2015).
7. Silva, N. F. D. *et al.* In situ formation of gold nanoparticles in polymer inclusion membrane: Application as platform in a label-free potentiometric immunosensor for Salmonella typhimurium detection. *Talanta* **194,** 134–142 (2019).
8. FDA. The reportable food registry: A five year overview of targeting inspection resources and identifying patterns of adulteration. *U.S. Food Drug Adm.* (2016).
9. Rapini, R. & Marrazza, G. Electrochemical aptasensors for contaminants detection in food and environment: Recent advances. *Bioelectrochemistry* **118,** 47–61 (2017).
10. Bobrinetskiy, I. I. & Knezevic, N. Z. Graphene-based biosensors for on-site detection of contaminants in food. *Anal. Methods* **10,** 5061–5070 (2018).
11. Das, S. R. *et al.* 3D nanostructured inkjet printed graphene: Via UV-pulsed laser irradiation enables paper-based electronics and electrochemical devices. *Nanoscale* **8,** 15870–15879 (2016).
12. Lin, J. *et al.* Laser-induced porous graphene films from commercial polymers. *Nat. Commun.* **5,** 1–8 (2014).
13. Chen, Y. *et al.* UV laser-induced polyimide to graphene conversion: modeling, fabrication, and application. *Small Methods* (2019). doi:10.1002/smtd.201900208
14. Rathinam, K. *et al.* Polyimide derived laser-induced graphene as adsorbent for cationic and anionic dyes. *Carbon N. Y.* **124,** 515–524 (2017).

15. Ye, R., James, D. K. & Tour, J. M. Laser-Induced Graphene. *Acc. Chem. Res.* **51,** 1609–1620 (2018).
16. Xu, M., Wang, R. & Li, Y. Rapid detection of Escherichia coli O157:H7 and Salmonella Typhimurium in foods using an electrochemical immunosensor based on screen-printed interdigitated microelectrode and immunomagnetic separation. *Talanta* **148,** 200–208 (2016).
17. Silva, N. F. D. *et al.* In situ formation of gold nanoparticles in polymer inclusion membrane: Application as platform in a label-free potentiometric immunosensor for Salmonella typhimurium detection. *Talanta* **194,** 134–142 (2019).
18. Alexandre, D. L. *et al.* A Rapid and Specific Biosensor for Salmonella Typhimurium Detection in Milk. *Food Bioprocess Technol.* **11,** 748–756 (2018).
19. Balandin, A. A. Thermal properties of graphene and nanostructured carbon materials. *Nat. Mater.* **10,** 569–581 (2011).
20. Wang, Y., Ye, Z. & Ying, Y. New trends in impedimetric biosensors for the detection of foodborne pathogenic bacteria. *Sensors* **12,** 3449–3471 (2012).
21. Novoselov, K. S. *et al.* Electric Field Effect in Atomically Thin Carbon Films. *Science (80-.).* **306,** 666–669 (2004).
22. Wang, F. *et al.* Laser-induced graphene: preparation, functionalization and applications. *Mater. Technol.* **33,** 340–356 (2018).
23. Stoller, M. D., Park, S., Zhu, Y., An, J. & Ruoff, R. S. Graphene-Based Ultracapacitors. 6–10 (2008).
24. Kurra, N., Jiang, Q., Nayak, P. & Alshareef, H. N. Laser-derived graphene: A three-dimensional printed graphene electrode and its emerging applications. *Nano Today* **24,** 81–102 (2019).
25. Nayak, P., Kurra, N., Xia, C. & Alshareef, H. N. Highly Efficient Laser Scribed Graphene Electrodes for On-Chip Electrochemical Sensing Applications. *Adv. Electron. Mater.* **2,** (2016).
26. Tehrani, F. & Bavarian, B. Facile and scalable disposable sensor based on laser engraved graphene for electrochemical detection of glucose. *Sci. Rep.* **6,** (2016).
27. Dorothee, G., Robert, M., Janos, V. & Erik, R. Electrochemical Biosensors - Sensor Principles and Architectures. *Sensors* **8,** 1400–1458 (2008).
28. Zhang, W. *et al.* 3D Laser Scribed Graphene Derived from Carbon Nanospheres: An

Ultrahigh-Power Electrode for Supercapacitors. *Small Methods* **3,** (2019).

29. Zhang, Z. *et al.* Visible light laser-induced graphene from phenolic resin: A new approach for directly writing graphene-based electrochemical devices on various substrates. *Carbon N. Y.* **127,** 287–296 (2018).
30. Torrisi, F. *et al.* Inkjet-printed graphene electronics. *ACS Nano* **6,** 2992–3006 (2012).
31. Yan, Z. *et al.* Toward the synthesis of wafer-scale single-crystal graphene on copper foils. *ACS Nano* **6,** 9110–9117 (2012).
32. Yan, Z. *et al.* Growth of Bilayer graphene on insulating substrates. *ACS Nano* **5,** 8187–8192 (2011).
33. Lin, J. *et al.* Laser-induced porous graphene films from commercial polymers. *Nat. Commun.* **5,** 1–8 (2014).
34. Duy, L. X. *et al.* Laser-induced graphene fibers. *Carbon N. Y.* **126,** 472–479 (2018).
35. El-Kady, M. F., Veronica, S., Sergey, D. & Richard, B. K. Laser Scribing of High-Performance. *Science (80-.).* **335,** 1326–1330 (2012).
36. Abramova, V., Slesarev, A. S. & Tour, J. M. Meniscus-mask lithography for narrow graphene nanoribbons. *ACS Nano* **7,** 6894–6898 (2013).
37. Abbas, A. N. *et al.* Patterning, characterization, and chemical sensing applications of graphene nanoribbon arrays down to 5 nm using helium ion beam lithography. *ACS Nano* **8,** 1538–1546 (2014).
38. Park, J. B., Yoo, J. H. & Grigoropoulos, C. P. Multi-scale graphene patterns on arbitrary substrates via laser-assisted transfer-printing process. *Appl. Phys. Lett.* **101,** (2012).
39. Chyan, Y. *et al.* Laser-Induced Graphene by Multiple Lasing: Toward Electronics on Cloth, Paper, and Food. *ACS Nano* **12,** 2176–2183 (2018).
40. Kumar, P. *et al.* Novel Radiation-Induced Properties of Graphene and Related Materials. *Chem. Synth. Appl. graphene carbon Mater.* 159–189 (2016). doi:10.1002/9783527648160.ch8
41. Zhang, J. *et al.* Efficient Water-Splitting Electrodes Based on Laser-Induced Graphene. *ACS Appl. Mater. Interfaces* **9,** 26840–26847 (2017).
42. Huang, T. *et al.* The effects of low power density CO2 laser irradiation on graphene properties. *Appl. Surf. Sci.* **273,** 502–506 (2013).
43. Lin, Z. *et al.* Precise control of the number of layers of graphene by picosecond laser

thinning. *Sci. Rep.* **5,** 1–7 (2015).

44. Arul, R. *et al.* The mechanism of direct laser writing of graphene features into graphene oxide films involves photoreduction and thermally assisted structural rearrangement. *Carbon N. Y.* **99,** 423–431 (2016).
45. Xu, S. C. *et al.* Direct synthesis of graphene on any nonmetallic substrate based on KrF laser ablation of ordered pyrolytic graphite. *Laser Phys. Lett.* **11,** (2014).
46. Park, J. B. *et al.* Fast growth of graphene patterns by laser direct writing. *Appl. Phys. Lett.* **98,** 16–19 (2011).
47. Lee, J., Lee, J., Koo, J. & Lee, J. H. Graphite saturable absorber based on the pencil-sketching method for Q-switching of an erbium fiber laser. *Appl. Opt.* **55,** 303 (2016).
48. Seo, B. H., Youn, J. & Shim, M. Direct laser writing of air-stable p-n junctions in graphene. *ACS Nano* **8,** 8831–8836 (2014).
49. Wen, W., Yan, X., Zhu, C., Du, D. & Lin, Y. Recent Advances in Electrochemical Immunosensors. *Am. Chem. Soc.* **89,** 138–156 (2016).
50. Vanegas, D. C. *et al.* Laser scribed graphene biosensor for detection of biogenic amines in food samples using locally sourced materials. *Biosensors* **8,** (2018).
51. Loo, A. H., Bonanni, A. & Pumera, M. Biorecognition on graphene: Physical, covalent, and affinity immobilization methods exhibiting dramatic differences. *Chem. - An Asian J.* **8,** 198–203 (2013).
52. Kaushik, S., Tiwari, U. K., Pal, S. S. & Sinha, R. K. Rapid detection of Escherichia coli using fiber optic surface plasmon resonance immunosensor based on biofunctionalized Molybdenum disulfide (MoS2) nanosheets. *Biosens. Bioelectron.* **126,** 501–509 (2019).
53. LaGraff, J. R. & Chu-LaGraff, Q. Scanning force microscopy and fluorescence microscopy of microcontact printed antibodies and antibody fragments. *Langmuir* **22,** 4685–4693 (2006).
54. Wacker, R., Schröder, H. & Niemeyer, C. M. Performance of antibody microarrays fabricated by either DNA-directed immobilization, direct spotting, or streptavidin-biotin attachment: A comparative study. *Anal. Biochem.* **330,** 281–287 (2004).
55. Peluso, P. *et al.* Optimizing antibody immobilization strategies for the construction of protein microarrays. *Anal. Biochem.* **312,** 113–124 (2003).
56. Zacco, E., Pividori, M. I. & Alegret, S. Electrochemical biosensing based on universal

affinity biocomposite platforms. *Biosens. Bioelectron.* **21,** 1291–1301 (2006).

57. Sung, W. J. & Bae, Y. H. Glucose oxidase, lactate oxidase, and galactose oxidase enzyme electrode based on polypyrrole with polyanion/PEG/enzyme conjugate dopant. *Sensors Actuators, B Chem.* **114,** 164–169 (2006).
58. Karyakin, A. A., Presnova, G. V., Rubtsova, M. Y. & Egorov, A. M. Oriented immobilization of antibodies onto the gold surfaces via their native thiol groups. *Anal. Chem.* **72,** 3805–3811 (2000).
59. Abdelbasir, S. M. *et al.* Graphene-Anchored Cuprous Oxide Nanoparticles from Waste Electric Cables for Electrochemical Sensing. *ACS Sustain. Chem. Eng.* **6,** 12176–12186 (2018).
60. Nguyen, P. D., Tran, T. B., Nguyen, D. T. X. & Min, J. Magnetic silica nanotube-assisted impedimetric immunosensor for the separation and label-free detection of Salmonella typhimurium. *Sensors Actuators, B Chem.* **197,** 314–320 (2014).
61. Katz, E. & Willner, I. Probing Biomolecular Interactions at Conductive and Semiconductive Surfaces by Impedance Spectroscopy: Routes to Impedimetric Immunosensors, DNA-Sensors, and Enzyme Biosensors. *Electroanalysis* **15,** 913–947 (2003).
62. Bonanni, A., Loo, A. H. & Pumera, M. Graphene for impedimetric biosensing. *TrAC - Trends Anal. Chem.* **37,** 12–21 (2012).
63. Li, G. *et al.* Generation of Small Single Domain Nanobody Binders for Sensitive Detection of Testosterone by Electrochemical Impedance Spectroscopy. *ACS Appl. Mater. Interfaces* **8,** 13830–13839 (2016).
64. Bhardwaj, S. K. *et al.* Immunosensing of Atrazine with Antibody-Functionalized Cu-MOF Conducting Thin Films. *ACS Appl. Mater. Interfaces* **7,** 26124–26130 (2015).
65. Wan, J. *et al.* Signal-off impedimetric immunosensor for the detection of Escherichia coli O157:H7. *Sci. Rep.* **6,** 2–7 (2016).
66. Sergi Brosel-Oliu, Uria, N., Abramova, N. & Bratov, A. Impedimetric Sensors for Bacteria Detection. *Intech* **9,** 257–288 (2015).
67. Bahadir, E. B. & Sezgintürk, M. K. A review on impedimetric biosensors. *Artif. Cells, Nanomedicine Biotechnol.* **44,** 248–262 (2014).
68. Grossi, M., Lanzoni, M., Lazzarini, R. & Riccò, B. Linear non iterative sinusoidal fitting algorithm for microbial impedance biosensor. *Sensors and Transducers* **137,**

235–244 (2012).

69. Ruecha, N., Shin, K., Chailapakul, O. & Rodthongkum, N. Label-free paper-based electrochemical impedance immunosensor for human interferon gamma detection. *Sensors Actuators, B Chem.* **279,** 298–304 (2019).
70. Lee, J. A. *et al.* An electrochemical impedance biosensor with aptamer-modified pyrolyzed carbon electrode for label-free protein detection. *Sensors Actuators, B Chem.* **129,** 372–379 (2008).
71. Pagliarini, V. *et al.* Treated Gold Screen-Printed Electrode as Disposable Platform for Label-Free Immunosensing of Salmonella Typhimurium. *Electrocatalysis* (2018). doi:10.1007/s12678-018-0491-1
72. Carvalho, L. A. De, Bueno, P. R., Química, I. De, Paulista, U. E. & Sp, A. Espectroscopia De Impedância Eletroquímica Aplicada Ao Estudo Das Reações. *Quim. Nova* **29,** 796–804 (2006).
73. Prodromidis, M. I. Impedimetric Biosensors and Immunosensors. *Pakistan J. Anal. Environ. Chem.* **8,** 69–71 (2007).
74. UN/DESA. World Population Prospects 2017 – Data Booklet (ST/ESA/SER.A/401). *United Nations, Dep. Econ. Soc. Aff. Popul. Div.* 1–24 (2017).
75. Hoffmann, S., Maculloch, B. & Batz, M. B. Economic Burden of Major Foodborne Illnesses Acquired in the United States. *Econ. Inf. Bull.* 59 (2015).
76. Punbusayakul, N., Talapatra, S., Ajayan, P. M. & Surareungchai, W. Label-free as-grown double wall carbon nanotubes bundles for Salmonella typhimurium immunoassay. *Chem. Cent. J.* **7,** 1–8 (2013).
77. Rotariu, L., Lagarde, F., Jaffrezic-Renault, N. & Bala, C. Electrochemical biosensors for fast detection of food contaminants - trends and perspective. *TrAC - Trends Anal. Chem.* **79,** 80–87 (2016).
78. Ping, J. *et al.* Recent advances in aptasensors based on graphene and graphene-like nanomaterials. *Biosens. Bioelectron.* **64,** 373–385 (2015).
79. Craciun, M. F., Russo, S., Yamamoto, M. & Tarucha, S. Tuneable electronic properties in graphene. *Nano Today* **6,** 42–60 (2011).
80. Lee, J.-H., Park, S. & Choi, J.-W. Electrical Property of Graphene and Its Application to Electrochemical Biosensing. *Nanomaterials* **9,** 297 (2019).
81. El-Kady, M. F., Strong, V., Dubin, S. & Kaner, R. B. Laser Scribing of High-

Performance and Flexible Graphene-Based Electrochemical Capacitors. *Science (80-.).* **335,** 1326–1330 (2012).

82. Quiton, P. A., Carreon, B. M., Cruz-papa, D. M. Dela & Bergantin, J. Bacteriophage-modified Graphene Oxide Screen-printed Electrodes for the Impedimetric Biosensing of Salmonella Enterica Serovar Typhimurium. *Sensors & Transducers* **28,** 38–42 (2018).
83. Khan, N. I., Maddaus, A. G. & Song, E. A low-cost inkjet-printed aptamer-based electrochemical biosensor for the selective detection of lysozyme. *Biosensors* **8,** (2018).
84. Rahimi, R., Ochoa, M., Yu, W. & Ziaie, B. Highly stretchable and sensitive unidirectional strain sensor via laser carbonization. *ACS Appl. Mater. Interfaces* **7,** 4463–4470 (2015).
85. Li, L. *et al.* High-Performance Pseudocapacitive Microsupercapacitors from Laser-Induced Graphene. *Adv. Mater.* **28,** 838–845 (2016).
86. Zhang, C. *et al.* Monolithic and Flexible ZnS/SnO 2 Ultraviolet Photodetectors with Lateral Graphene Electrodes. *Small* **13,** 1–7 (2017).
87. Tao, L. Q. *et al.* An intelligent artificial throat with sound-sensing ability based on laser induced graphene. *Nat. Commun.* **8,** 1–8 (2017).
88. Fenzl, C. *et al.* Laser-Scribed Graphene Electrodes for Aptamer-Based Biosensing. *ACS Sensors* **2,** 616–620 (2017).
89. Muniandy, S. *et al.* A reduced graphene oxide-titanium dioxide nanocomposite based electrochemical aptasensor for rapid and sensitive detection of Salmonella enterica. *Bioelectrochemistry* **127,** 136–144 (2019).
90. Nicholson, R. S. Theory and Application of Cyclic Voltammetry for Measurement of Electrode Reaction Kinetics. *Anal. Chem.* **37,** 1351–1355 (1965).
91. Taguchi, M. *et al.* PulSED: Pulsed sonoelectrodeposition of fractal nanoplatinum for enhancing amperometric biosensor performance. *Analyst* **141,** 3367–3378 (2016).
92. Nguyen, V. T. *et al.* Synthesis of multi-layer graphene films on copper tape by atmospheric pressure chemical vapor deposition method. *Adv. Nat. Sci. Nanosci. Nanotechnol.* **4,** 2–7 (2013).
93. Pimenta, M. A. *et al.* Studying disorder in graphite-based systems by Raman spectroscopy. *Phys. Chem. Chem. Phys.* **9,** 1276–1291 (2007).

94. Wang, Q. H. *et al.* Understanding and controlling the substrate effect on graphene electron-transfer chemistry via reactivity imprint lithography. *Nat. Chem.* **4,** 724–732 (2012).
95. Griffiths, K. *et al.* Laser-scribed graphene presents an opportunity to print a new generation of disposable electrochemical sensors. *Nanoscale* **6,** 13613–13622 (2014).
96. B. Oliveira, S. C. & Oliveira-Brett, A. M. Voltammetric and electrochemical impedance spectroscopy characterization of a cathodic and anodic pre-treated boron doped diamond electrode. *Electrochim. Acta* **55,** 4599–4605 (2010).
97. Katz, E., Lioubashevsky, O. & Willner, I. Electromechanics of a Redox-Active Rotaxane in a Monolayer Assembly on an Electrode. *J. Am. Chem. Soc.* **126,** 15520–15532 (2007).
98. Li, Y. & Chen, S. M. The electrochemical properties of acetaminophen on bare glassy carbon electrode. *Int. J. Electrochem. Sci.* **7,** 2175–2187 (2012).
99. Ambrosi, A., Bonanni, A., Sofer, Z., Cross, J. S. & Pumera, M. Electrochemistry at chemically modified graphenes. *Chem. - A Eur. J.* **17,** 10763–10770 (2011).
100. Ohk, S. H., Koo, O. K., Sen, T., Yamamoto, C. M. & Bhunia, A. K. Antibody-aptamer functionalized fibre-optic biosensor for specific detection of Listeria monocytogenes from food. *J. Appl. Microbiol.* **109,** 808–817 (2010).
101. Ding, S. *et al.* Rapid and Label-Free Detection of Interferon Gamma via an Electrochemical Aptasensor Comprising a Ternary Surface Monolayer on a Gold Interdigitated Electrode Array. *ACS Sensors* **2,** 210–217 (2017).
102. Mutreja, R. *et al.* Novel surface antigen based impedimetric immunosensor for detection of Salmonella typhimurium in water and juice samples. *Biosens. Bioelectron.* **85,** 707–713 (2016).
103. Farka, Z. *et al.* Rapid Immunosensing of Salmonella Typhimurium Using Electrochemical Impedance Spectroscopy: the Effect of Sample Treatment. *Electroanalysis* **28,** 1803–1809 (2016).
104. Salam, F. & Tothill, I. E. Detection of Salmonella typhimurium using an electrochemical immunosensor. *Biosens. Bioelectron.* **24,** 2630–2636 (2009).

APPENDIX

Experimental Details

All statistical analysis and grahing was performed using JMP v.13 Software (SAS Institute, USA) and SiglmaPlot 12 software, respectively. The electroactive surface area (*ESA or A*) was calculated from CV curves using Equation 1 (Randles-Sevcik equation).

$$I_p = 2.69 \times 10^5 A D^{1/2} n^{3/2} \nu^{1/2} C \quad (1)$$

where I_p is the oxidation/reduction peak obtained from the CV curves (ampere), A is the electroactive surface area (cm^2), D is the coefficient of diffusion ($cm^2\ s^{-1}$), n is the number of transferred electrons in the redox reaction, ν is the scan rate ($V\ s^{-1}$), and C is the concentration of the redox probe ($mol\ cm^{-3}$).

The heterogeneous electron transfer rate (HET) represented by the constant (k^0) was calculated according to Nicholson method for reversible electron tranfers[90] through Equation 2 used to calculate the dimensionless kinetic parameter (Ψ), dependent on ΔE_p.

$$\Psi = k^0 \left(\frac{D_o}{D_r}\right)^{\alpha/2} \sqrt{\frac{RT}{nFD_o\nu\pi}} \quad (2)$$

where D_o/D_r is the ratio of diffusion coefficients of the oxidized and reduced forms of the electroactive species, α is the transfer coefficient, R is the universal gas constant (8.314 $J\ K^{-1}\ mol^{-1}$), T is the absolute temperature, n is the number of electrons transferred in the electrochemical reaction, F is the Faraday constant (96489 $C\ mol^{-1}$), ν is the scan rate in $V\ s^{-1}$. Considering $D_o \approx D_r$ and the redox kinetics approximately symmetric, it means $\alpha \approx 0$, Equation 2 can be simplified to Equation 3.

$$\Psi = k^0 \sqrt{\frac{RT}{FD\nu\pi}} \quad (3)$$

Since this is a one electron process, Ψ depends on ΔE_p and can be determined from the Equation 4 below, where X is equal to the peak potential separation (ΔE_p) of the system multiplied by the number of electrons involved in the electrochemical reaction (n). Therefore k^0 could be determined[25].

$$\Psi = \frac{-0.6288 + 0.0021\,X}{1 - 0.017\,X} \tag{4}$$

The 3σ method was used to calculate the limit of detection (LOD)[50,91] and to predict about the sensitivity, using the Equation 5 below, where y_b is the value for the blank (charge transfer resistance of BPW or chicken broth without bacteria), SD is the standard deviation (n = 3), y_0 is the y-intercept, and sensitivity represents the slope from change in charge transfer resistance (ΔR_{ct}) *versus* bacteria concentration. The reproducibility at different bacteria concentrations was evaluated by repeating the experiment three times using three different working electrodes.

$$LOD = \frac{(y_b + 3\,SD) - y_0}{sensitivity} \tag{5}$$